Inorg. Chem. **2005**, *44*, 8937–8946

A Family of Oxo-Chalcogenide Molybdenum and Tungsten Complexes, (n-$Bu_4N)_2[M_2O_2(\mu$-$Q)_2$(1,3-dithiole-2-thione-4,5-dithiolate)$_2$] (M = Mo, W; Q = S, Se): New Synthetic Entries, Structure, and Gas-Phase Behavior

Rosa Llusar,*,† Sonia Triguero,† Cristian Vicent,† Maxim N. Sokolov,‡ Benoît Domercq,§ and Marc Fourmigué§

Departament de Ciències Experimentals, Universitat Jaume I, Campus de Riu Sec, P.O. Box 224, 12080 Castelló, Spain, Nikolayev Institute of Inorganic Chemistry SB RAS, pr. Lavrentyeva 3, 630090 Novosibirsk, Russia, and Laboratoire CIMMA, UMR 6200 CNRS-Université d'Angers, UFR Sciences Bât. K, 2 Bd. Lavoisier, 49045 Angers, France

Received May 31, 2005

A new series of complexes with the general formula (n-$Bu_4N)_2[M_2O_2(\mu$-$Q)_2$(dmit)$_2$] (where M = Mo, W; Q = S, Se; dmit = 1,3-dithiole-2-thione-4,5-dithiolate) have been prepared. Fragmentation of the trinuclear cluster (n-$Bu_4N)_2$-$[Mo_3(\mu_3$-$S)(\mu$-$S_2)_3$(dmit)$_3$] in the presence of triphenylphosphine (PPh_3) gives the dinuclear compound (n-$Bu_4N)_2$-$[Mo_2O_2(\mu$-$S)_2$(dmit)$_2$] {(n-$Bu_4N)_2$[**2**]}, which is formed via oxidation in air from the intermediate (n-$Bu_4N)_2[Mo_3(\mu_3$-$S)(\mu$-$S)_3$(dmit)$_3$] {(n-$Bu_4N)_2$[**1**]} complex. Ligand substitution of the molybdenum sulfur bridged $[Mo_2O_2(\mu$-$S)_2$(dimethylformamide)$_6]^{2+}$ dimer with the sodium salt of the dmit dithiolate also affords the dianionic compound (n-$Bu_4N)_2$[**2**]. The whole series, (n-$Bu_4N)_2[Mo_2O_2(\mu$-Se$)_2$(dmit)$_2$] {(n-$Bu_4N)_2$[**3**]}, (n-$Bu_4N)_2[W_2O_2(\mu$-S$)_2$(dmit)$_2$] {(n-$Bu_4N)_2$[**4**]}, (n-$Bu_4N)_2[W_2O_2(\mu$-Se$)_2$(dmit)$_2$] {(n-$Bu_4N)_2$[**5**]}, and (n-$Bu_4N)_2[Mo_2O_2(\mu$-S$)_2$(dmid)$_2$] {(n-$Bu_4N)_2$[**6**]; dmid = 1,3-dithiole-2-one-4,5-dithiolate}, has been synthesized by the excision of the polymeric $(Mo_3Q_7Br_4)_x$ phases with PPh_3 or 1,2-bis(diphenylphosphanyl)ethane in acetonitrile followed by the dithiolene incorporation and further degradation in air. Direct evidence of the presence of the intermediates with the formula $[M_3Q_4$(dmit)$_3]^{2-}$ (M = Mo, W; Q = S, Se) has been obtained by electrospray ionization mass spectrometry. The crystal structures of (n-$Bu_4N)_2$[**1**], $(PPh_4)_2[Mo_2O_2(\mu$-S$)_2$(dmit)$_2$] {$(PPh_4)_2$[**2**]; PPh_4 = tetraphenylphosphonium}, (n-$Bu_4N)_2$[**2**], (n-$Bu_4N)_2$[**4**], $(PPh_4)_2[W_2O_2(\mu$-Se$)_2$(dmit)$_2$] {$(PPh_4)_2$[**5**]}, and (n-$Bu_4N)_2$[**6**] have been determined. A detailed study of the gas-phase behavior for compounds (n-$Bu_4N)_2$[**2**–**6**] shows an identical fragmentation pathway for the whole family that consists of a partial breaking of the two dithiolene ligands followed by the dissociation of the dinuclear cluster.

Introduction

The bioinorganic significance of oxo-dithiolene molybdenum and tungsten complexes is well-known, and it has been put forward that, specifically, the $[MO(1,2\text{-dithiolene})_2]^-$ (M = Mo, W) compounds can serve as molecular models for the active sites of several enzyme families, such as the dimethyl sulfoxide reductases and aldehyde ferredoxin oxidoreductase.[1,2] In addition, 1,2-dithiolene complexes provide numerous opportunities in solid-state chemistry as molecular conductors or as nonlinear optical materials.[3−7] With this regard, homoleptic 1,2-dithiolene mononuclear complexes are known as bis- or tris-dithiolene complexes, with square-planar or trigonal-prismatic geometries, where their redox and optical properties can be carefully tuned within the series

* To whom correspondence should be addressed. E-mail: llusar@exp.uji.es.
† Universitat Jaume I.
‡ Nikolayev Institute of Inorganic Chemistry SB RAS.
§ Université d'Angers.

(1) Johnson, M. K.; Rees, D. C.; Adams, M. W. W. *Chem. Rev.* **1996**, *96*, 2817.
(2) McMaster, J.; Tunney, J. M.; Garner, C. D. Chemical Analogues of the Catalytic Centers of Molybdenum and Tungsten Dithiolene-Containing Enzymes. *Dithiolene Chemistry, Synthesis, Properties and Applications*; John Wiley & Sons: Hoboken, NJ, 2004; Vol. 52, p 539.
(3) Cassoux, P.; Valade, L.; Kobayashi, H.; Kobayashi, A.; Clark, R. A.; Underhill, A. E. *Coord. Chem. Rev.* **1991**, *110*, 115.
(4) Fourmigue, M. *Coord. Chem. Rev.* **1998**, *178*, 823.
(5) Allen, A. E.; Olk, R. M. *Coord. Chem. Rev.* **1999**, *188*, 211.
(6) Matsubayashi, G.; Nakano, M.; Tamura, H. *Coord. Chem. Rev.* **2002**, *226*, 143.
(7) Faulmann, C.; Cassoux, P. Solid State Properties (Electronic, Magnetic, Optical) of dithiolene Complexes-Based Compounds. *Dithiolene Chemistry, Synthesis, Properties and Applications*; John Wiley & Sons: Hoboken, NJ, 2004; Vol. 52, p 399.

10.1021/ic0508728 CCC: $30.25
Published on Web 10/22/2005

by varying the metal, the substituents, and the redox state. In particular, the coordination of dmit (1,3-dithiole-2-thione-4,5-dithiolate) to Ni, Pd, or Pt has been especially fruitful and resulted in the discovery of the first inorganic superconductor in the salt tetrathiafulvalene (TTF)$[Ni(dmit)_2]_2$.[8] Since then an enormous interest has been launched in the study of other dithiolene ligands coordinated to less usual systems, including "f-" or "p-block" elements.[9−11] In contrast, the use of polynuclear units combined with these ligands has been scarcely studied mainly as a result of the lack of rational synthetic entries to this class of compounds. In some cases self-assembly methodologies starting from low nuclearity complexes have proven to be a convenient entry to dithiolene-containing clusters, for example, those containing a cubane-type Fe_4S_4 structure.[12,13] Remarkably, the ability of the dithiolene ligands to coordinate in different fashions yields interesting and unexpected polynuclear complexes with dithiolene-bridged ligands, for example, the dinuclear rhenium $(PPh_4)_2[Re_2(\mu\text{-dmit})(dmit)_4]$ (PPh_4 = tetraphenylphosphonium) compound or several tetranuclear complexes, that is, $Au_4(\mu\text{-dmit})_2(\mu\text{-dppm})_2$, and $(Me_4N)_2\{Cu_4[4,5\text{-(methylsulfanyl)}_2\text{-}TTF_3]\}$.[14−16] Therefore, the development of rational entries to 1,2-bis(dithiolene) cluster compounds remains a field to be explored.

Recently, our group has reported the synthesis of the dmit-containing trinuclear cluster $[Mo_3S_7(dmit)_3]^{2-}$ by the substitution of the labile bromine ligands in the $[Mo_3S_7Br_6]^{2-}$ precursor. The resulting compound can be oxidized to afford the corresponding neutral complex that exhibits high conductivity and an antiferromagnetic behavior.[17] In this work, we extend our research on group VI chalcogenide clusters, focusing on the fragmentation of these trinuclear species to afford oxo-dinuclear complexes containing the dmit ligand. Up to now, a number of dmit-dinuclear complexes have been reported, for example, the tto-bridged dimers (tto = tetrathiooxalate, $C_2S_4^{2-}$) of formula $[D]_x\{tto[M(dmit)]_2\}$ (D = *n*-Bu_4N, Et_4N, Me_4N; M = Ni, Cu), the dmit-bridged complexes such as $(PPh_4)_2[Re_2(\mu\text{-dmit})_2(dmit)_3]$ and $(n\text{-}Bu_4N)_2[Ni_2(\mu\text{-dmit})_2(dmit)]$, or the halogen-bridged $(n\text{-}Bu_4N)_2[Pt_2(\mu\text{-X})(dmit)_2]$ (X = Cl, Br, SPh) dimetallic compounds.[14,18−22] However, dmit-coordinated dimetallic complexes with halogen or chalcogen bridges are quite scarce, even though complexes with $[M(\mu\text{-}X)_2M]$ centers (X = Cl, Br, O, S) are very common in coordination chemistry.

Herein, we report new synthetic approaches to the oxomolybdo- and tungsten-bis(dithiolene) complexes on the basis of the degradation of trinuclear clusters $[M_3Q_7]$ in the presence of a reducing reagent. Electrospray ionization mass spectrometry (ESI-MS) has been used to identify the intermediates involved in such degradations. In the case of molybdenum, the more direct ligand substitution approach on the dinuclear $[Mo_2O_2(\mu\text{-}S)_2(DMF)_6]I_2$ (DMF = dimethylformamide) complex has been explored. Although ESI-MS is becoming a powerful tool to characterize dithiolene-containing complexes and monitor their reactivities,[23,24] studies based on tandem MS are lacking so far in this field. Mononuclear dithiolene-containing clusters have been investigated by ESI-MS using "in-source fragmentation", where the observed peaks correspond to different partial dissociations of the ligand; however, no mechanism could be proposed for the fragmentation process on the basis of only those experiments.[23] The use of tandem MS makes a mechanism proposal feasible because it provides additional information about the structure and reactivity of the ionized target molecule in the gas phase through the fragmentation paths observed in the collision-induced dissociation (CID) spectra. For instance, the redox interconversion in solution between Fe_4S_4 and Fe_2S_2 assemblies has been proven to occur also in the gas phase.[25,26]

In this work, we describe the first tandem ESI-MS investigations on 1,2-dithiolene-containing di- and trinuclear complexes in the pure gas phase that show the existence of a well-defined fragmentation pathway for the $(n\text{-}Bu_4N)_2[M_2O_2(\mu_2\text{-}Q)_2(dmit)_2]$ series. The mechanism occurs via two consecutive ruptures of the dmit ligand (evolving CS_2 and $C_2S_2^-$), which results in the species formulated as $[M_2O_2(\mu\text{-}Q)_2S_2]^-$, followed by a symmetric degradation to give the mononuclear $[MOSQ_{bridged}]^-$ species.

Experimental Section

General Procedures. All reactions were carried out in air unless otherwise stated. The polymeric phases $(M_3Q_7Br_4)_x$ (M = Mo, W; Q = S, Se) and the complexes $[Mo_2O_2(\mu\text{-}S)_2(DMF)_6]I_2$, $(n\text{-}Bu_4N)_2[Mo_3S_7(dmit)_3]$, $[M_3Q_4Br_3(dppe)_3]PF_6$ [M = Mo, W; Q = S, Se; dppe = 1,2-bis(diphenylphosphanyl)ethane], and $(n\text{-}Bu_4N)_2[Zn(dithiolene)_2]$ (dithiolene = dmit, dmid; dmid = 1,3-dithiole-2-one-4,5-dithiolate) were prepared according to literature methods.[17,27−29] $Na_2(dmit)$ salt was prepared by reacting $dmit(COPh)_2$ (1.22 g, 3

(8) Bousseau, M.; Valade, L.; Legros, J. P.; Cassoux, P.; Garbauskas, M.; Interrante, L. V. *J. Am. Chem. Soc.* **1986**, *108*, 1908.
(9) Roger, M.; Arliguie, T.; Thuery, P.; Fourmigue, M.; Ephritikhine, M. *Inorg. Chem.* **2005**, *44*, 584.
(10) Roger, M.; Arliguie, T.; Thuery, P.; Fourmigue, M.; Ephritikhine, M. *Inorg. Chem.* **2005**, *44*, 594.
(11) Avarvari, N.; Fourmigue, M. *Organometallics* **2003**, *22*, 2042.
(12) Inomata, S.; Tobita, H.; Ogino, H. *J. Am. Chem. Soc.* **1990**, *112*, 6145.
(13) Inomata, S.; Tobita, H.; Ogino, H. *Inorg. Chem.* **1992**, *31*, 723.
(14) Matsubayashi, G.; Maikawa, T.; Tamura, H.; Nakano, M.; Arakawa, R. *J. Chem. Soc., Dalton Trans.* **1996**, 1539.
(15) Cerrada, E.; Laguna, A.; Laguna, M.; Jones, P. G. *J. Chem. Soc., Dalton Trans.* **1994**, 1325.
(16) Dai, J.; Munakata, M.; Ohno, Y.; Bian, G. Q.; Suenaga, Y. *Inorg. Chim. Acta* **1999**, *285*, 332.
(17) Llusar, R.; Uriel, S.; Vicent, C.; Coronado, E.; Gomez-Garcia, C. J.; Clemente-Juan, J. M.; Braida, B.; Canadell, E. *J. Am. Chem. Soc.* **2004**, *126*, 12076.
(18) Pullen, A. E.; Zeltner, S.; Olk, R.-M.; Hoyer, E.; Abboud, K. A.; Reynolds, J. R. *Inorg. Chem.* **1996**, *35*, 4420.
(19) Pullen, A. E.; Olk, R.-M.; Zeltner, S.; Hoyer, E.; Abboud, K. A.; Reynolds, J. R. *Inorg. Chem.* **1997**, *36*, 958.
(20) Pullen, A. E.; Zeltner, S.; Olk, R.-M.; Hoyer, E.; Abboud, K. A.; Reynolds, J. R. *Inorg. Chem.* **1997**, *36*, 4163.
(21) Breitzer, J. G.; Rauchfuss, T. *Polyhedron* **2000**, *19*, 1283.
(22) Dai, J.; Bian, G.-Q.; Zhou, M.-Y.; Zhu, Q.-Y.; Guo, L.; Zhang, J.-S. *Synth. Met.* **2004**, *140*, 53.
(23) Falaras, P.; Mitsopoulou, C. A.; Argyropoulos, D.; Lyris, E.; Psaroudakis, N.; Vrachnou, E.; Katakis, D. *Inorg. Chem.* **1995**, *34*, 4536.
(24) Dessapt, R.; Simmonet-Jegat, C.; Mallard, A.; Lavanant, H.; Marrot, J.; Secheresse, F. *Inorg. Chem.* **2003**, *42*, 6424.
(25) Yang, X.; Wang, X.-B.; Niu, S.; Pickett, C. J.; Ichiye, T.; Wang, L.-S. *Phys. Rev. Lett.* **2002**, *89*, 163401.
(26) Yang, X.; Wang, X.-B.; Wang, L.-S. *Int. J. Mass Spectrom.* **2003**, *228*, 797.
(27) Coucouvanis, D.; Toupadakis, A.; Lane, J. D.; Koo, S. M.; Kim, C. G.; Hadjikyriacou, A. *J. Am. Chem. Soc.* **1991**, *113*, 5271.

mmol) with sodium methanolate (×2) in methanol. After precipitation with diethyl ether, the desired violet salt is obtained in a quantitative yield. The remaining reactants were obtained from commercial sources and used as received. Solvents for the synthesis were dried and degassed by standard methods before use. Chromatographic work was performed on silica gel, 60 Å. IR spectra were recorded in the 300−3500 cm^{-1} range on a Perkin-Elmer system 2000 Fourier transform infrared spectrometer using KBr pellets. Raman spectra were recorded on a Perkin-Elmer system 2000 Fourier transform near-infrared instrument equipped with a diode-pumped Nd:YAG laser PSU. The position of the sample was manually adjusted for each case to obtain the maximum intensity for a laser power of 700 mW.

ESI-MS. A Quattro LC (quadrupole−hexapole−quadrupole) mass spectrometer with an orthogonal Z-spray electrospray interface (Micromass, Manchester, U.K.) was used. Sample solutions in acetonitrile (approximately 5×10^{-5} M) were infused via syringe pump directly to the interface at a flow rate of 10 μL/min. The temperature of the source block was set to 100 °C, and the interface temperature was set to 150 °C. A capillary voltage of 3.5 kV was used in the negative scan mode, and the cone voltage was kept at 20 V to avoid fragmentation of the molecular ions. The drying gas, as well as the nebulizing gas, was nitrogen set at flow rates of 400 and 80 L/h, respectively. The chemical composition of each peak in the scan mode was assigned by comparison of the isotope experimental pattern with that calculated using the MassLynx 3.5 program. The CID spectra were obtained at various collision energies (CEs; typically varied from 0 to 70 eV) by selecting the precursor ion of interest with MS1 and scanning MS2 at a cone voltage kept at 20 V. Argon or synthetic air (70% N_2 and 30% O_2) was used as the collision gas, and the pressure in the collision cell was maintained at 1×10^{-3} mbar. When multiple-stage tandem MS^3 experiments were carried out, the cone voltage was varied to generate the desired parent ion. In both cases, the isolation width in the first quadrupole was 1 Da.

Synthesis. Preparation of $(n\text{-}Bu_4N)_2[Mo_3S_4(dmit)_3]$ {$(n\text{-}Bu_4N)_2$-[**1**]}. Triphenylphosphine (PPh_3; 0.03 g, 0.11 mmol) was added to a violet solution of $(n\text{-}Bu_4N)_2[Mo_3S_7(dmit)_3]$ (0.05 g, 0.03 mmol) in 10 mL of CH_2Cl_2 under nitrogen. An immediate color change was observed from violet to red. The solution was stirred for 10 min, and the desired compound $(n\text{-}Bu_4N)_2$[**1**] was precipitated with diethyl ether. The precipitate was separated from the solution by filtration under an inert atmosphere, was washed thoroughly with toluene and diethyl ether to eliminate the PPh_3S, and was recrystallized from CH_2Cl_2/diethyl ether mixtures (0.024 g, 52%). Anal. Calcd for $Mo_3S_{19}C_{41}H_{72}N_2$: C, 33.05; H, 4.87; S, 40.88; N, 1.88. Found: C, 33.03; H, 4.96; S, 40.97; N, 1.92. IR (KBr, cm^{-1}): 1459 [s, ν(C═C)]; 1054 [vs, ν(C═S)]; 512 [m, ν(C−S)]; 469 (m), 316 (m), ν(Mo−S_{dmit}) and ν[Mo−(μ-S)]. Raman (cm^{-1}): 1421 [m, ν(C═C)]; 999 [m, ν(C═S)]; 512 [w, ν(C−S)]; 470 (w), 363(w), 315 (w), ν(Mo−S_{dmit}) and ν[Mo−(μ-S)]; 259 {w, ν[Mo−(μ_3-S)]}. ESI-MS(−) *m*/*z*: 503 $[M]^{2-}$.

Preparation of $(n\text{-}Bu_4N)_2[Mo_2O_2(\mu\text{-}S)_2(dmit)_2]$ {$(n\text{-}Bu_4N)_2$[**2**]}. Method 1. To a solution of $[Mo_2O_2(\mu\text{-}S)_2(DMF)_6]I_2$ (prepared in situ from 1 g of $Mo_2O_2(\mu\text{-}S)_2(S_2)_2$ and 0.8 g of iodine in DMF) was added an excess of Na_2dmit (0.70 g, 2.89 mmol). After stirring overnight, the addition of 50 mL of an aqueous solution containing $(n\text{-}Bu_4N)$Br (0.70 g, 2.89 mmol) caused the precipitation of an orange solid which was washed with 10 mL of CS_2, 10 mL of ethanol, and diethyl ether. Recrystallization from acetonitrile/ethanol afforded the desired compound $(n\text{-}Bu_4N)_2$[**2**] (1.25 g; 72%).

Method 2. A violet solution of $(n\text{-}Bu_4N)_2[Mo_3S_7(dmit)_3]$ (0.10 g, 0.06 mmol) in acetonitrile (20 mL) was allowed to react with PPh_3 (0.05 g, 0.18 mmol) for 1 day. The resulting dark-brown solution was evaporated under reduced pressure, redissolved in CH_2Cl_2, and loaded onto a silica-gel column. After washing with CH_2Cl_2, elution with acetone yielded a concentrated brown solution that was taken to dryness. The resulting solid was recrystallized from CH_2Cl_2/diethyl ether mixtures to give $(n\text{-}Bu_4N)_2$[**2**] (0.06 g; 82%). Anal. Calcd for $Mo_3S_{12}C_{38}H_{72}N_2O_2$: C, 39.15; H, 6.23; S, 33.01; N, 2.40. Found: C, 39.12; H, 5.97; S, 32.82; N, 2.40. IR (KBr, cm^{-1}): 1460 [m, ν(C═C)]; 1053 [vs, ν(C═S)]; 944 [m, ν(Mo═O)]; 508 [m, ν(C−S)]; 464 (m), 316 (m), ν(Mo−S_{dmit}) and ν[Mo−(μ-S)]. Raman (cm^{-1}): 1414 [s, ν(C═C)]; 1009 [m, ν(C═S)]; 932 [m, ν(Mo═O)]; 508 [m, ν(C−S)]; 474 (w), 367 (w), ν(Mo−S_{dmit}) and ν[Mo−(μ-S)]. ESI-MS(−) *m*/*z*: 340 $[M]^{2-}$.

Preparation of $(n\text{-}Bu_4N)_2[Mo_2O_2(\mu\text{-}Se)_2(dmit)_2]$ {$(n\text{-}Bu_4N)_2$[**3**]}. Method 1. The polymer $(Mo_3Se_7Br_4)_x$ (0.12 g, 0.10 mmol) was reacted with PPh_3 (0.08 g, 0.30 mmol) in acetonitrile (25 mL) in the presence of $(n\text{-}Bu_4N)_2[Zn(dmit)_2]$ (0.14 g, 0.15 mmol) under reflux conditions for 2 days. The resulting dark-brown solution was filtered, taken to dryness, and purified following the chromatographic workup described for compound $(n\text{-}Bu_4N)_2$[**2**]. The final complex $(n\text{-}Bu_4N)_2$[**3**] was obtained as a brown solid (0.013 g; 10%).

Method 2. A solution of $[Mo_3Se_4(dppe)_3Br_3]PF_6$ (0.15 g, 0.07 mmol) and $(n\text{-}Bu_4N)_2[Zn(dmit)_2]$ (0.10 g, 0.11 mmol) in acetonitrile (25 mL) was allowed to react in air at room temperature for 1 day. The resulting dark-brown solution was evaporated under reduced pressure, redissolved in dichloromethane, and purified as described for $(n\text{-}Bu_4N)_2$[**2**] (0.02 g; 22%). Anal. Calcd for $Mo_3S_{10}Se_2C_{38}$-$H_{72}N_2O_2$: C, 36.24; H, 5.76; S, 25.46; N, 2.22. Found: C, 36.16; H, 5.81; S, 25.32; N, 2.27. IR (KBr, cm^{-1}): 1433 [m, ν(C═C)]; 1054 [s, ν(C═S)]; 943 [m, ν(Mo═O)]; 514 [m, ν(C−S)]; 481 (w), 328 (w), ν(Mo−S_{dmit}) and ν[Mo−(μ-Se)]. Raman (cm^{-1}): 1436 [s, ν(C═C)]; 1000 [m, ν(C═S)]; 932 [w, ν(Mo═O)]; 472 (w), 372 (w), 325 (w), ν(Mo−S_{dmit}) and ν[Mo−(μ-Se)]. ESI-MS(−) *m*/*z*: 390 $[M]^{2-}$.

Preparation of $(n\text{-}Bu_4N)_2[W_2O_2(\mu\text{-}S)_2(dmit)_2]$ {$(n\text{-}Bu_4N)_2$[**4**]}. Compound $(n\text{-}Bu_4N)_2$[**4**] was prepared following the procedures described for $(n\text{-}Bu_4N)_2$[**3**] but starting from $(W_3S_7Br_4)_x$ (0.50 g, 0.45 mmol), PPh_3 (0.35 g, 1.30 mmol), and $(n\text{-}Bu_4N)_2[Zn(dmit)_2]$ (0.64 g, 0.69 mmol) for method 1 and $[W_3S_4(dppe)_3Br_3]PF_6$ (0.14 g, 0.06 mmol) with $(n\text{-}Bu_4N)_2[Zn(dmit)_2]$ (0.09 g, 0.09 mmol) for method 2. In both cases, the resulting dark-brown product was obtained in 20% yields. Anal. Calcd for $W_3S_{12}C_{38}H_{72}N_2O_2$: C, 34.02; H, 5.41; S, 28.68; N, 2.40. Found: C, 34.13; H, 5.31; S, 28.54; N, 2.12. IR (KBr, cm^{-1}): 1460 [m, ν(C═C)]; 1053 [vs, ν-(C═S)]; 956 [m, ν(W═O)]; 525 [m, ν(C−S)]; 468 (m), 441 (w), ν(W−S_{dmit}) and ν[W−(μ-S)]. Raman (cm^{-1}): 1417 [s, ν(C═C)]; 1035 [w, ν(C═S)]; 937 [m, ν(W═O)]; 517 [w, ν(C−S)]; 474 (w), 374 (w), ν(W−S_{dmit}) and ν[W−(μ-S)]. ESI-MS(−) *m*/*z*: 428 $[M]^{2-}$.

Preparation of $(n\text{-}Bu_4N)_2[W_2O_2(\mu\text{-}Se)_2(dmit)_2]$ {$(n\text{-}Bu_4N)_2$[**5**]}. Compound $(n\text{-}Bu_4N)_2$[**5**] was prepared as described for complex $(n\text{-}Bu_4N)_2$[**3**] but starting from $(W_3Se_7Br_4)_x$ (0.50 g, 0.35 mmol), PPh_3 (0.28 g, 1.05 mmol), and $(n\text{-}Bu_4N)_2[Zn(dmit)_2]$ (0.50 g, 0.51 mmol) for method 1 and $[W_3Se_4(dppe)_3Br_3]PF_6$ (0.15 g, 0.06 mmol) with $(n\text{-}Bu_4N)_2[Zn(dmit)_2]$ (0.09 g, 0.095 mmol) for method 2. The final brown product was obtained in 30 and 15% yields by methods 1 and 2, respectively. Anal. Calcd for $W_3S_{10}Se_2C_{38}H_{72}N_2O_2$: C, 31.80; H, 5.06; S, 22.34; N, 1.95. Found: C, 31.76; H, 5.16; S,

(28) Feliz, M.; Llusar, R.; Uriel, S.; Vicent, C.; Humphrey, M. G.; Lucas, N. T.; Samoc, M.; Luther-Davies, B. *Inorg. Chim. Acta* **2003**, *349*, 69.

(29) Müller, H.; Molina, A. P.; Narymbetov, B. Z.; Zorina, L. V.; Khasanov, S. S.; Shibaeva, R. P. *Z. Anorg. Allg. Chem*. **1998**, *624*, 1492.

Table 1. Crystallographic Data for $(n\text{-}Bu_4N)_2$[**1**], $(PPh_4)_2$[**2**], $(n\text{-}Bu_4N)_2$[**2**], $(n\text{-}Bu_4N)_2$[**4**], $(PPh_4)_2$[**5**], and $(n\text{-}Bu_4N)_2$[**6**]

compound	$(n\text{-}Bu_4N)_2$[**1**]	$(PPh_4)_2$[**2**]	$(n\text{-}Bu_4N)_2$[**2**]	$(n\text{-}Bu_4N)_2$[**4**]	$(PPh_4)_2$[**5**]	$(n\text{-}Bu_4N)_2$[**6**]
empirical formula	$C_{41}H_{72}Mo_3N_2S_{19}$	$C_{54}H_{40}O_2P_2S_{12}Mo_2$	$C_{38}H_{72}Mo_2N_2O_2S_{12}$	$C_{38}H_{72}N_2O_2S_{12}W_2$	$C_{54}H_{40}O_2P_2S_{10}Se_2W_2$	$C_{38}H_{72}N_2O_4S_{10}Mo_2$
formula weight	1489.97	1359.40	1165.58	1341.40	1629.02	1133.46
crystal system	monoclinic	monoclinic	orthorhombic	orthorhombic	monoclinic	monoclinic
a (Å)	9.210(4)	11.920(6)	17.9420(12)	18.0620(13)	11.942(2)	22.770(5)
b (Å)	36.769(18)	22.899(12)	15.9050(16)	15.9787(12)	22.855(5)	13.988(3)
c (Å)	19.382(10)	20.951(11)	19.1558(17)	19.2806(14)	20.851(4)	19.668(4)
β (deg)	103.331(11)	98.689(13)			96.340(5)	121.029(5)
V (Å^3)	6387(5)	5653(5)	5466.4(8)	5564.5(7)	5655.9(19)	5368(2)
T (K)	233(2)	293(2)	293(2)	293(2)	293(2)	293(2)
space group	$P2(1)/c$	$P2(1)/c$	$Pbcn$	$Pbcn$	$P2(1)/c$	$C2/c$
Z	4	4	4	4	4	4
μ(Mo Kα) (mm^{-1})	1.231	0.985	0.949	4.613	5.818	0.892
reflections collected	20 889	24 842	37 585	23 706	25 287	12 335
ϕ range for data collection (deg)	1.11−21.50	1.73−22.50	2.41−28.08	1.70−25.00	1.33−22.50	1.79−23.00
unique reflections	7275	7365	6529	4899	7371	3734
R (int)	0.1857	0.1239	0.1973	0.1576	0.1670	0.0993
goodness-of-fit on F^2	1.309	1.011	0.768	1.203	0.961	0.965
R1[a]	0.1262	0.0674	0.0495	0.0860	0.0665	0.0516
wR2[b]	0.2588	0.1496	0.0696	0.2129	0.1428	0.1149
R1[a] (all data)	0.2282	0.1469	0.1846	0.1794	0.1690	0.1205
wR2[b] (all data)	0.2983	0.1853	0.0945	0.2669	0.1951	0.1488
residual ρ (e Å^{-3})	1.220 and −0.968	0.720 and −0.874	0.447 and −0.298	2.060 and −2.045	1.061 and −1.573	0.716 and −0.349

[a] $R1 = \sum||F_o| - |F_c||/\{\sum F_o\}$. [b] $wR2 = [\sum[w(F_o^2 - F_c^2)^2]/\sum[w(F_o^2)^2]^{1/2}$.

22.77; N, 1.96. IR (KBr, cm^{-1}): 1467 [m, ν(C═C)]; 1067 [vs, ν(C═S)]; 960 [m, ν(W═O)]; 510 [m, ν(C−S)]; 469 (w), 449(w), 320 (w), ν(W−S_{dmit}) and ν[W−(μ-Se)]. Raman (cm^{-1}): 1425 [s, ν(C═C)]; 1054 [w, ν(C═S)]; 957 [m, ν(W═O)]; 468 (w), 365 (w), 257 (w), ν(W−S_{dmit}) and ν[W−(μ-Se)]. ESI-MS(−) m/z: 476 $[M]^{2-}$.

Preparation of $(n\text{-}Bu_4N)_2[Mo_2O_2(\mu\text{-}S)_2(dmid)_2]$ {$(n\text{-}Bu_4N)_2$[**6**]}. Compound $(n\text{-}Bu_4N)_2$[**6**] was prepared following the procedure described in method 1 for compound $(n\text{-}Bu_4N)_2$[**3**] but starting from $(Mo_3S_7Br_4)_x$ (0.05 g, 0.06 mmol), PPh_3 (0.05 g, 0.18 mmol), and $(n\text{-}Bu_4N)_2[Zn(dmid)_2]$ (0.08 g, 0.09 mmol). The resulting dark-brown product was obtained in 82% yield. Anal. Calcd for $Mo_3S_{10}C_{38}H_{72}N_2O_4$: C, 40.26; H, 6.40; S, 28.29; N, 2.47. Found: C, 40.21; H, 6.23; S, 28.85; N, 2.42. IR (KBr, cm^{-1}): 1663 (s), 1613 (s), ν(C═O); 1437 [m, ν(C═C)]; 945 [m, ν(Mo═O)]; 527 [m, ν(C−S)]; 465 (w), 447 (w), 340 (w), ν(Mo−S_{dmid}) and ν[Mo−(μ-S)]. The Raman spectra of compound $(n\text{-}Bu_4N)_2$[**6**] gave broad signals centered around 1600 and 930 cm^{-1}, which is a sign of overheating or burning up, thus, precluding a reliable analysis. ESI-MS(−) m/z: 325 $[M]^{2-}$.

X-ray Crystallography. Suitable crystals for X-ray studies for compounds $(n\text{-}Bu_4N)_2$[**1**], $(PPh_4)_2[Mo_2O_2(\mu\text{-}S)_2(dmit)_2]$ {$(PPh_4)_2$-[**2**]}, $(n\text{-}Bu_4N)_2$[**4**], $(PPh_4)_2[W_2O_2(\mu\text{-}Se)_2(dmit)_2]$ {$(PPh_4)_2$[**5**]}, and $(n\text{-}Bu_4N)_2$[**6**] were grown by the slow diffusion of diethyl ether into sample solutions in CH_2Cl_2, while crystals of $(n\text{-}Bu_4N)_2$[**2**] were obtained by the recrystallization of acetonitrile/methanol mixtures. In the case of complex $(n\text{-}Bu_4N)_2$[**1**], crystals were grown under nitrogen in a drybox. Replacement of the $(n\text{-}Bu_4N)^+$ cation in $[\mathbf{2}]^{2-}$ and $[\mathbf{5}]^{2-}$ was done by the addition of an excess of PPh_4Br to hot methanol solutions of the dianions that precipitate the desired PPh_4 salts. The data collection for compound $(n\text{-}Bu_4N)_2$[**2**] was carried out on a Stoe imaging plate diffraction system (IPDS) using graphite-monochromated Mo Kα radiation ($\lambda = 0.710\ 73$ Å) with a crystal-to-detector distance of 70 mm and a ϕ increment of 1.3°. The data collection for $(n\text{-}Bu_4N)_2$[**1**], $(PPh_4)_2$[**2**], $(n\text{-}Bu_4N)_2$[**4**], $(PPh_4)_2$[**5**], and $(n\text{-}Bu_4N)_2$[**6**] was performed on a Bruker Smart charge-coupled device diffractometer using graphite-monochromated Mo Kα radiation ($\lambda = 0.710\ 73$ Å) with a nominal crystal-to-detector distance of 4 cm. A hemisphere of data were collected on the basis of three ω-scan runs (starting with $\omega = -28°$) at values $\phi = 0°$, 90°, and 180° with the detector at $2\theta = 28°$. At each of these runs, frames (606, 435, and 230, respectively) were collected at 0.3° intervals and 35 s per frame for compounds $(n\text{-}Bu_4N)_2$[**1**], $(PPh_4)_2$[**2**], $(n\text{-}Bu_4N)_2$[**4**], $(PPh_4)_2$[**5**], and $(n\text{-}Bu_4N)_2$[**6**]. The diffraction frames were integrated using the SAINT package and corrected for absorption with SADABS.[30,31] The crystal parameters and basic information relating the data collection and the structure refinement for the three compounds are summarized in Table 1.

In all six compounds, the positions of the heavy atoms were determined by direct methods, and successive difference electron density maps using the SHELXTL 5.10 software package were done to locate the remaining atoms.[32] Refinement was performed by the full-matrix least-squares method based on F^2. All atoms except carbon from the tetrabutylammonium groups in $(n\text{-}Bu_4N)_2$[**1**] and $(n\text{-}Bu_4N)_2$[**4**] were refined anisotropically. Some of the terminal carbon atoms in the tetrabutylammonium cations in compound $(n\text{-}Bu_4N)_2$[**1**] appeared disordered in two positions, in particular C(110)−C(111) and C(214)−C(215), and their bond distances were constrained at a fixed value. In the same way, the bond distance between the C(20) and the C(21) carbon atoms of the tetrabutylammonium cation in compound $(n\text{-}Bu_4N)_2$[**4**] had to also be fixed. The tetrabutylammonium cation disorder in $(n\text{-}Bu_4N)_2$[**1**] and $(n\text{-}Bu_4N)_2$[**4**] results in goodness-of-fit values larger than unity and also in high R values (see Table 1); however, the geometry of the cluster anions in both structures is well-defined. The low goodness-of-fit values in $(n\text{-}Bu_4N)_2$[**2**] are due to a small crystal size combined with the specific treatment of the standard deviations of the intensities, as determined by the Stoe IPDS. All hydrogen atoms of the phenyl and butyl groups were generated geometrically.

Results and Discussion

Synthesis and ESI-MS. In the past decades, several synthetic approaches have evolved that are different from the nonrational self-assembly processes for the preparation

(30) *Saint*, 5.0 ed.; Bruker Analytical X-Ray Systems: Madison, WI, 1996.
(31) Sheldrick, G. M. *SADABS*; empirical absorption program; University of Göttingen: Göttingen, Germany, 1996.
(32) Sheldrick, G. M. *SHELXTL*, 5.1 ed.; Bruker Analytical X-Ray Systems: Madison, WI, 1997.

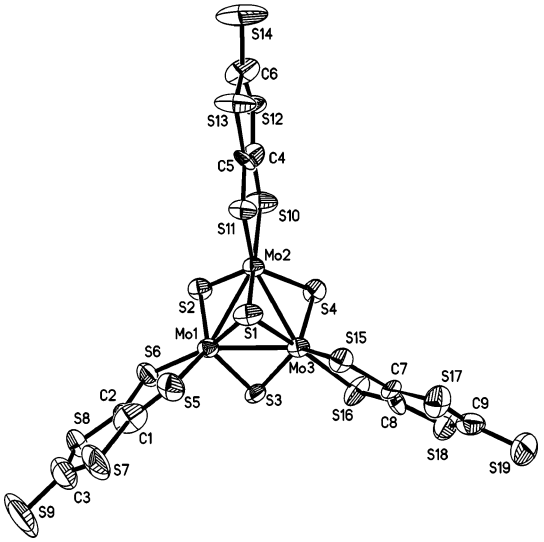

Figure 1. ORTEP representation (50% ellipsoid probability) of the dianion $[\mathbf{1}]^{2-}$. Selected average bond distances for Mo−Mo, 2.767[6]; Mo−[μ_3-S(1)], 2.355[9]; Mo−(μ-S), 2.28[2]; Mo−[S_L trans to μ_3-S(1)], 2.479[4]; and Mo−(S_L trans to μ-S), 2.368[5]. Standard deviations of the averaged values are given in brackets.

Scheme 1. Reaction Scheme of the Synthetic Strategies Employed in the Preparation of $[Mo_3S_4(dmit)_3]^{2-}$ ($[\mathbf{1}]^{2-}$) and $[Mo_2O_2(\mu\text{-}S)_2(dmit)_2]^{2-}$ ($[\mathbf{2}]^{2-}$)

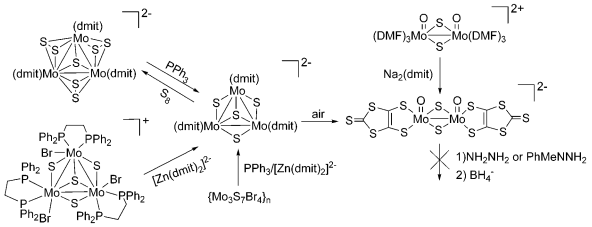

of transition metal cluster complexes. One of these strategies consists of the fragmentation of clusters of higher nuclearity. We have observed that the reaction of the trinuclear Mo(IV) complex (n-$Bu_4N)_2[Mo_3S_7(dmit)_3]$ in the presence of PPh_3 results in an immediate color change from violet to red, and ESI-MS shows $[Mo_3S_4(dmit)_3]^{2-}$ as the only reaction product. This anion is very air-sensitive in solution, and its degradation in air results in the formation (yield = 82%) of well-defined products of the formula (n-$Bu_4N)_2[\mathbf{2}]$. Alternatively, this complex can be obtained starting from the preassembled dimer $[Mo_2O_2(\mu\text{-}S)_2(DMF)_6]I_2$ by the substitution of the labile DMF ligands with the dmit dithiolate in 72% yields. Scheme 1 illustrates the reactions involved.

The intermediate (n-$Bu_4N)_2[\mathbf{1}]$ is formed by the reduction of the bridging disulfides in the precursor (n-$Bu_4N)_2[Mo_3S_7(dmit)_3]$. Although complex ($n$-$Bu_4N)_2[\mathbf{1}]$ is extremely air-sensitive in solution, the solid samples can be handled in air for several hours. The ORTEP diagram of the $[\mathbf{1}]^{2-}$ dianion is shown in Figure 1.

Compound (n-$Bu_4N)_2[\mathbf{1}]$ represents a rare example, only observed before in the $[Mo_3S_4(S_2C_2H_4)_3]^{2-}$ complex, where each molybdenum(IV) atom appears pentacoordinated, if one ignores the metal−metal bond, instead of its more common octahedral environment.[33] The Mo_3S_4 cluster core is nearly identical to that previously found in $[Mo_3S_4(S_2C_2H_4)_3]^{2-}$ with an equilateral triangle of Mo(IV) atoms bound by Mo−Mo bonds of 2.760(3)−2.772(4) Å, a single capping μ_3 sulfido S(1), and three bridging μ-sulfido ligands, S(2), S(3), and S(4). The pentacoordinated environment of each metal is completed by a chelating dmit ligand. Selected bond distances for $[\mathbf{1}]^{2-}$ are given in Figure 1. Raman and infrared spectra of compound (n-$Bu_4N)_2[\mathbf{1}]$ show the characteristic signals of the trinuclear Mo_3S_4 cluster unit [medium intensity frequencies in the 259−470 cm^{-1} range attributed to the Mo−(μ-S) and Mo−(μ_3-S) stretching vibrations][34,35] and the absence of bands due to the S_2^{2-} bridges found in the starting precursor (n-$Bu_4N)_2[Mo_3S_7(dmit)_3]$ at about 550 cm^{-1}.[17] The use of PPh_3 as a desulfurizing reagent on related Mo_3S_7 complexes has been previously reported by Fedin et al., showing that such abstraction involves the removal of three equatorial sulfur atoms and, in contrast with the present case, is always accompanied by the filling of the resulting coordination vacancy to produce an octahedral environment around the molybdenum atoms.[34,35]

The use of ESI-MS as a tool for the rapid characterization of related compounds has been recently reported.[24] This technique appears to be particularly suitable for the MS analysis of the dianionic complexes (n-$Bu_4N)_2[\mathbf{1}]$ and (n-$Bu_4N)_2[\mathbf{2}]$, as it provides an avenue for the rapid monitoring of chemical modifications in the cluster unit. Figure 2 shows the ESI-MS spectra of the reaction mixture recorded at different intervals.

Complete oxidation of the anion $[\mathbf{1}]^{2-}$ takes place within about 1 h with the concomitant appearance of the dimer $[\mathbf{2}]^{2-}$. On the basis of the almost quantitative formation of $[\mathbf{2}]^{2-}$, we postulate that fragmentation occurs according to the scheme $[Mo^{IV}_3(\mu_3\text{-}S)(\mu\text{-}S)_3] \rightarrow [Mo^{V}_2O_2(\mu\text{-}S)_2] + [Mo]$, although the mononuclear species could not be detected by ESI-MS. In addition, no oxo-trinuclear intermediates, that is, the hypothetical species $[Mo_3S_4O(dmit)_3]^{2-}$ and $[Mo_3S_4O_2(dmit)_3]^{2-}$, could be identified by ESI-MS, presumably because oxygen uptake in solution results in a rapid breaking and rearrangement of the metallic cluster to give the dinuclear complexes. In most cases the detailed mechanism of oxygen transfers is very difficult to elucidate, mainly because the oxygen transfer to transition metal compounds by dioxygen or by single oxygen atoms results in species with different reactivities and whose transient nature precludes their characterization. This problem can be easily overcome by transferring the metal or oxo-metal complex to the gas phase and then studying its ion−molecule reactivity.[36−38] Following this procedure, the cluster $[Mo_3S_4(dmit)_3]^{2-}$ ($[\mathbf{1}]^{2-}$) was mass-selected in the first quadrupole and then collided with air (1×10^{-3} mbar) in the collision cell at CEs ranging from $E_{lab} = 0$ to $E_{lab} = 15$ eV. This low CE was used to avoid

(33) Halbert, T. R.; McGauley, K.; Pan, W. H.; Czernuszewicz, R. S.; Stiefel, E. I. *J. Am. Chem. Soc.* **1984**, *106*, 1849.
(34) Fedin, V. P.; Kolesov, B. A.; Mironov, Y. V.; Fedorov, V. Y. *Polyhedron* **1989**, *8*, 2419.
(35) Fedin, V. P.; Sokolov, M. N.; Mironov, Y. V.; Kolesov, B. A.; Tkachev, S. V.; Fedorov, V. Y. *Inorg. Chim. Acta* **1990**, *167*, 39.
(36) Plattner, D. A. *Int. J. Mass Spectrom.* **2001**, *207*, 125.
(37) Feichtinger, D.; Plattner, D. A. *Angew. Chem., Int. Ed. Engl.* **1997**, *36*, 1718.
(38) Feichtinger, D.; Plattner, D. A. *J. Chem. Soc., Perkin Trans.* **2000**, *2*, 1023.

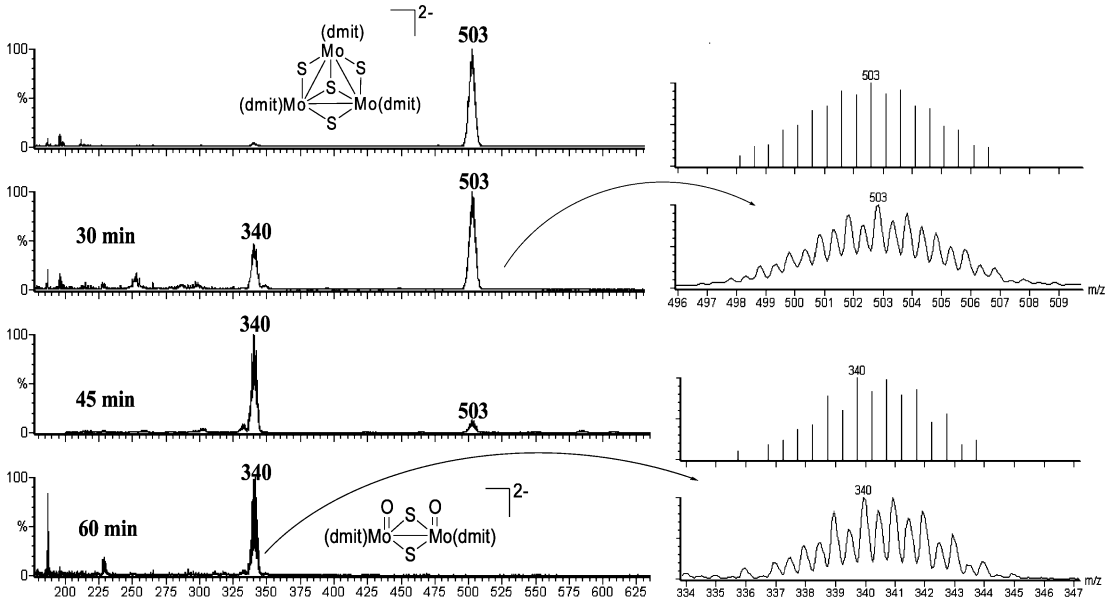

Figure 2. Mass spectra recorded immediately after the addition of 3 equiv of PPh_3 to the trinuclear $[Mo_3S_7(dmit)_3]^{2-}$ cluster (top) and after allowing the mixture to stand in air for 30, 45, and 60 min. The insets show the simulated and experimental peaks corresponding to $[Mo_3S_4(dmit)_3]^{2-}$ (centered at m/z = 503 amu) and $[Mo_2O_2(\mu\text{-}S)_2(dmit)_2]^{2-}$ (centered at m/z = 340 amu).

fragmentation at the same time as maximizing the residence time of the target ion in the collision cell. In this experiment the intact cluster $[\mathbf{1}]^{2-}$ was the only peak observed even after increasing the pressure in the cell up to 3×10^{-2} mbar. These experimental results suggest that oxygen uptake is presumably slow and, therefore, could be tentatively proposed as the limiting step in the degradation of the trinuclear unit.

The anion $[\mathbf{1}]^{2-}$ can also be obtained by the substitution of the diphosphine and the bromide ligands by the dmit dithiolate in the air-stable $[Mo_3S_4(dppe)_3Br_3]^{+}$ trinuclear cation, which is obtained by the cluster excision of the $(Mo_3S_7Br_4)_x$ polymer by dppe, as represented in Scheme 1. Alternatively, the $[\mathbf{1}]^{2-}$ cluster dianion can be prepared in a one-pot reaction starting from the $(Mo_3S_7Br_4)_x$ cluster polymer and the dmit source, namely, $[Zn(dmit)_2]^{2-}$, in the presence of a desulfurizing agent such as PPh_3. These two approaches have been extended for the preparation of the whole family of molybdenum and tungsten sulfido and selenido dmit derivatives of the formula $(n\text{-}Bu_4N)_2[\mathbf{3}]$, $(n\text{-}Bu_4N)_2[\mathbf{4}]$, and $(n\text{-}Bu_4N)_2[\mathbf{5}]$ and of the homologous molybdenum complex $(n\text{-}Bu_4N)_2[\mathbf{6}]$. Except for the $(n\text{-}Bu_4N)_2[\mathbf{6}]$ complex, which is prepared in a one-pot reaction starting from $(Mo_3S_7Br_4)_x$ in 82% yield, the yields obtained for the other complexes are considerably lower with values ranging between 10 and 20%. In all cases, the reaction monitoring by ESI-MS shows the formation of the pentacoordinated intermediates $[M_3Q_4(\text{dithiolene})_3]^{2-}$ (M = Mo, W; Q = S, Se; dithiolene = dmit, dmid) as the product previous to the degradation. The presence of the three vacant positions can be associated with the observed high reactivity versus O_2 in complexes $[M_3Q_4(dmit)_3]^{2-}$ (M = Mo, W; Q = S, Se) and $[Mo_3S_4(S_2C_2H_4)_3]^{2-}$. Recently, a new method, namely, "cluster cracking", has been reported to prepare dmit-containing complexes in which the chelating ability of this ligand is used to break the cluster cores and form reassembled coordination compounds.[22,39] Our approach is slightly different because the breaking of the metal−metal bonds is due to metal oxidation rather than to the chelating ability of the dmit ligand. This route is especially valuable in the case of the selenium complexes $[\mathbf{3}]^{2-}$ and $[\mathbf{5}]^{2-}$ where the dinuclear precursors do not exist.

A similar oxidative fragmentation, $[Mo^{IV}_3(\mu_3\text{-}S)(\mu\text{-}S)_3] \rightarrow [Mo^{V}_2O_2(\mu\text{-}S)_2] + [Mo]$, was reported by Cotton et al. starting from cuboidal Mo_4S_4 aquo ions to give well-defined products, namely, $[Mo_3S_4(H_2O)_9]^{4+}$ or the dinuclear compound $[Mo_2O_2(\mu\text{-}S)_2(H_2O)_4]^{2+}$.[40] Incidentally, this fragmentation corresponds to the reverse of the synthesis of the cuboidal Mo_3S_4 and Mo_4S_4 complexes from dinuclear $Mo_2O_2(\mu\text{-}S)_2$ precursors in the presence of $NaBH_4$.[41,42] This inherent reactivity of oxo-dinuclear compounds to associate under reducing conditions leads us to explore this possibility as represented in Scheme 1. The action of $NaBH_4$ or $LiBH_4$ to $(n\text{-}Bu_4N)_2[\mathbf{2}]$ solutions in THF was checked by ESI-MS, and no reaction was detected. Also, the reaction of this $[\mathbf{2}]^{2-}$ complex with hydrazines, NH_2NH_2 or $PhMeNNH_2$, did not show the formation of the corresponding condensation product, as observed in related oxo-molybdenum or tungsten complexes.[43−45] Like compound $(n\text{-}Bu_4N)_2[\mathbf{2}]$, the complexes

(39) Dai, J.; Bian, G.-Q.; Wang, X.; Xu, Q.-F.; Zhou, M.-Y.; Munakata, M.; Maekawa, M.; Tong, M.-H.; Sun, Z.-R.; Zeng, H.-P. *J. Am. Chem. Soc.* **2000**, *122*, 11007.
(40) Cotton, F. A.; Dori, Z.; Llusar, R.; Schwotzer, W. *Inorg. Chem.* **1986**, *25*, 3654.
(41) Martinez, M.; Ooi, B.-L.; Sykes, A. G. *J. Am. Chem. Soc.* **1987**, *109*, 4615.
(42) Coyle, C. L.; Eriksen, K. A.; Farina, S.; Francis, J.; Gea, Y.; Greaney, M. A.; Guzi, P. J.; Halbert, T. R.; Murray, H. H.; Stiefel, E. I. *Inorg. Chim. Acta* **1992**, *198*, 565.
(43) Chatt, J.; Crichton, B. A. L.; Dilworth, J. R.; Dahlstrom, P.; Gutkoska, R.; Zubieta, J. *Inorg. Chem.* **1982**, *21*, 2383.
(44) Bustos, C.; Manzur, C.; Carrillo, D.; Robert, F. *Inorg. Chem.* **1994**, *33*, 1427.
(45) Masumori, T.; Seino, H.; Mizobe, Y.; Hidai, M. *Inorg. Chem.* **2000**, *39*, 5002.

Table 2. Selected Averaged Bond Distances (Å) for Compounds $(PPh_4)_2$[**2**], $(n\text{-}Bu_4N)_2$[**2**], $(n\text{-}Bu_4N)_2$[**4**], $(PPh_4)_2$[**5**], and $(n\text{-}Bu_4N)_2$[**6**][a]

	M—M (Å)	M—(μ-Q) range (Å)	M═O (Å)	M—S_{ligand} range (Å)	Π[b]	θ[c]	ref
$(PPh_4)_2$[**2**]	2.817(2)	2.342(3)−2.366(3)	1.678(7)−1.691(7)	2.425(4)−2.452(3)	135.9	19.9−24.7	this work
$(n\text{-}Bu_4N)_2$[**2**]	2.8223(12)	2.316(2)	1.658(3)	2.427(2)−2.436(2)	143.4	20.1	this work
$(n\text{-}Bu_4N)_2$[**4**]	2.825(2)	2.316(6)−2.329(6)	1.788(14)	2.429(6)−2.434(6)	141.8	18.9	this work
$(PPh_4)_2$[**5**]	2.8715(14)	2.434(3)−2.447(3)	1.700(15)−1.736(17)	2.406(8)−2.433(6)	135.5	15.3−25.5	this work
$(n\text{-}Bu_4N)_2$[**6**]	2.816(2)	2.326(3)−2.340(2)	1.665(5)	2.402(3)−2.429(2)	137.8	17.4	this work
$(NEt_4)_2[Mo_2O_2(\mu\text{-}S)_2\text{-}S_2C_2(COOMe)_2$	2.853(1)	2.327(3)−2.341(3)	1.671(6)−1.677(6)	2.408(3)−2.403(3)	148.0	3.9	70
$Mo_2O_2(\mu\text{-}S)_2\text{-}[S_2P(OEt)_2]_2$	2.828(3)	2.291(4)−2.322(5)	1.66(1)	2.466(4)−2.508(5)	149.3		50

[a] Standard deviations are given in parentheses. [b] Dihedral angle between the two M—(μ-S_2) planes. [c] Folding angle in the metallacycle $M_2S_2C_2$.

$(n\text{-}Bu_4N)_2$[**3**−**6**] do not react with sodium and lithium borohydride, NH_2NH_2, and $PhMeNNH_2$. ESI-MS monitoring of the reaction between $(n\text{-}Bu_4N)_2$[**1**] and sulfur showed the presence of an intact $(n\text{-}Bu_4N)_2$[**1**] together with the formation of small amounts of the $[Mo_3S_7(dmit)_3]^{2-}$ starting precursor.

Let us note that a terminal-sulfur-containing dinuclear compound, namely, $(PPh_4)_2[W_2S_2(\mu\text{-}S)_2(dmit)_2]$, has been previously described by Rauchfuss et al. as a subproduct in the reaction of $(PPh_4)_2[WS_4]$ with the thiocarbonyl of formula C_4OS_5, although only spectroscopic evidence were reported.[46] Complexes $[\mathbf{2}-\mathbf{6}]^{2-}$ with a $M_2O_2(\mu\text{-}Q)_2$ central unit can serve as precursors for the preparation of the corresponding $M_2S_2\text{-}(\mu\text{-}Q)_2$ derivatives by treatment with a sulfide reagent such as H_2S or $(Me_3Si)_2S$. Further investigations in this direction are in progress. Complexes with $M_2S_2(\mu\text{-}Q)_2$ units are of interest as templates for the preparation of heterobimetallic cubane-type complexes by the incorporation of metal fragments following the method originally developed by Stiefel and co-workers.[47]

Crystal Structures of $(PPh_4)_2$[2], $(n\text{-}Bu_4N)_2$[2], $(n\text{-}Bu_4N)_2$[4], $(PPh_4)_2$[5], and $(n\text{-}Bu_4N)_2$[6]. The structures of complexes $(PPh_4)_2$[**2**], $(n\text{-}Bu_4N)_2$[**2**], $(n\text{-}Bu_4N)_2$[**4**], $(PPh_4)_2\text{-}$[**5**], and $(n\text{-}Bu_4N)_2$[**6**] have been determined by single-crystal X-ray diffraction. Compounds $(PPh_4)_2$[**2**] and $(PPh_4)_2$[**5**] crystallize in the monoclinic space group $P2(1)/c$ and are isostructural. Complexes $(n\text{-}Bu_4N)_2$[**2**] and $(n\text{-}Bu_4N)_2$[**4**] are also isostructural and crystallize in the orthorhombic *Pbcn* group. These results anticipate the structural role played by the counterion in the final packing of these dmit-containing dimers. The dmid-containing compound $(n\text{-}Bu_4N)_2$[**6**] crystallizes in the monoclinic $C2/c$ space group. Figure 3 shows the ORTEP representation of the $[\mathbf{5}]^{2-}$ and $[\mathbf{6}]^{2-}$ dianions together with their atom-numbering scheme.

In all five structures the two metal centers are connected through two doubly bridged sulfide or selenido groups, where each metal atom appears five-coordinated without considering the metal−metal interaction. The remaining positions are occupied by the two sulfur atoms of the dithiolate ligand and a terminal oxygen atom in a square pyramidal environment. The oxygen atoms in complexes $(PPh_4)_2$[**2**], $(n\text{-}Bu_4N)_2\text{-}$[**2**], $(n\text{-}Bu_4N)_2$[**4**], $(PPh_4)_2$[**5**], and $(n\text{-}Bu_4N)_2$[**6**] are in a syn configuration. Metal atoms are located about 0.7 Å above

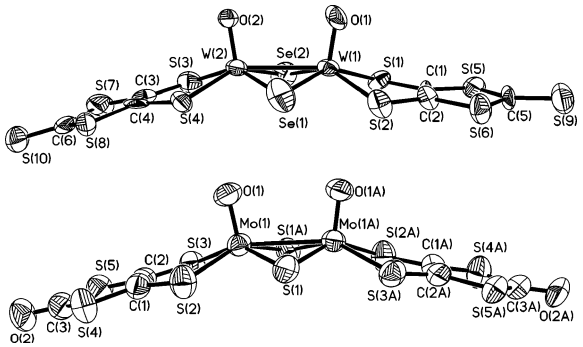

Figure 3. ORTEP representation (50% ellipsoid probability) of the dianion $[\mathbf{5}]^{2-}$ (top) and $[\mathbf{6}]^{2-}$ (bottom) with the atom numbering scheme. Symmetry transformations used to generate equivalent atoms (A) $1 - x, y$, and $-z + 1/2$.

the approximate square plane defined by the bridging chalcogenide and dithiolate sulfur atoms. This is a typical arrangement of molybdenum and tungsten dimers of the general formula $M_2X_2(\mu\text{-}Q)_2L_2$ (X = O, S, Se; Q = S, Se), where L represents a variety of terminal ligands such as dithiocarbamates, maleonitriledithiolate, dithiophosphates, mixed dithiolate and disulfide ligands, or polyselenides.[24,48−54] Table 2 shows a list of selected bond lengths together with those of other dinuclear complexes containing the same $M_2O_2(\mu\text{-}S)_2$ cluster core.

The M—M bond distances in these cluster anions are consistent with an oxidation state of +5 for the metal and the presence of a single metal−metal bond. The metal−metal bond distances in the sulfur-bridged complexes $(PPh_4)_2$[**2**], $(n\text{-}Bu_4N)_2$[**2**], $(n\text{-}Bu_4N)_2$[**4**], and $(n\text{-}Bu_4N)_2$[**6**] remain unchanged upon the substitution of Mo by W. The change of sulfur by selenium in these $[W_2O_2(\mu\text{-}Q)_2(dmit)_2]^{2-}$ anions increases by 0.06 Å the W—W bond lengths and is accompanied by a closure of the dihedral angle (Π) between the two W—(μ-Q)$_2$ planes. The replacement of Mo^V by W^V in the isostructural compounds $(n\text{-}Bu_4N)_2$[**2**] and $(n\text{-}Bu_4N)_2\text{-}$[**4**] also leaves unchanged the M—(μ-S) bond lengths, and the most significant difference is observed for the M═O

(46) Yang, X.; Freeman, G. K. W.; Rauchfuss, T. B.; Wilson, S. R. *Inorg. Chem.* **1991**, *30*, 3034.
(47) Halbert, T. R.; Cohen, S. A.; Stiefel, E. I. *Organometallics* **1985**, *4*, 1689.
(48) Howlader, N. C.; Haight, G. P., Jr.; Hambley, T. W.; Snow, M. R.; Lawrence, G. A. *Inorg. Chem.* **1984**, *23*, 1811.
(49) Gelder, J. I.; Enemark, J. H. *Inorg. Chem.* **1976**, *8*, 1839.
(50) Drake, J. E.; Mislankar, A. G.; Ratnani, R. *Inorg. Chem.* **1996**, *35*, 2665.
(51) Dessapt, R.; Simmonet-Jegat, C.; Marrot, J.; Secheresse, F. *Inorg. Chem.* **2001**, *40*, 4072.
(52) Lu, Y.-J.; Ansari, M. A.; Ibers, J. *Inorg. Chem.* **1989**, *38*, 4049.
(53) Wardle, R. W. L.; Bhaduri, S.; Chau, C.-N.; Ibers, J. *Inorg. Chem* **1988**, *27*, 1747.
(54) Seigneurin, A.; Makani, T.; Jones, D. J.; Rozière, J. *J. Chem. Soc., Dalton Trans.* **1987**, 1878.

distance, where an increase of about 0.13 Å is observed. Theoretical calculations predict a less pronounced increase in the M═O bond length upon metal substitution.[55] Changes in the outer ligand do not affect these M═O distances (see Table 2). In the case of the mononuclear dithiolene complexes of formula $[MO(dithiolene)_2]^{2-}$ (M = Mo, W), the M═O bond lengths are also slightly larger for the tungsten derivatives.[2] The W═O distance in $[\mathbf{4}]^{2-}$ decreases by 0.09 Å when sulfur is replaced by selenium.

In all cases, the $M_2S_2C_2$ metallacycle is folded along the S—S hinge. The folding angles θ observed for the dianions in the tetrabutylammonium salts are 20.1° for $[\mathbf{2}]^{2-}$, 17.4° for $[\mathbf{4}]^{2-}$, and 18.9° for $[\mathbf{6}]^{2-}$. The PPh_4 salts of the molybdenum sulfide and tungsten selenide dianions are slightly more distorted, with folding angles of 19.9 and 24.7° for $[\mathbf{2}]^{2-}$ and 15.3 and 25.5° for $[\mathbf{5}]^{2-}$. Incidentally, the lower Π dihedral angles correspond to these PPh_4^+ salts. For the tetraethylammonium salt of $Mo_2O_2(\mu\text{-}S)_2S_2C_2(COOMe)_2$, the angle $\theta = 3.9°$. No clear tendencies in this θ folding angle are observed upon substitution of the metal, bridging chalcogen, or outer dithiolene ligand. In consequence, the most significant differences in the θ folding angle can be associated with the counterion. Replacement of the counterion in mononuclear complexes containing dithiolene ligands is well-known to dramatically affect the folding angle along the dithiolene S—S hinge, thus, introducing an unpredictable distortion that can be at the origin of some unusual variations in the bond distances.[56]

Characteristic features of the infrared and Raman spectra of compounds $(n\text{-}Bu_4N)_2[M_2O_2(\mu\text{-}Q)_2(dmit)_2]$ (M = Mo, W; Q = S, Se), $(n\text{-}Bu_4N)_2[\mathbf{2}-\mathbf{5}]$, are given in Experimental Section. Besides the characteristic signals of the tetrabutylammonium cation, the most intense bands in the infrared spectra of these compounds are associated with the dmit ligands.[57] The complex $(n\text{-}Bu_4N)_2[\mathbf{6}]$ also shows two strong bands between 1640 and 1660 cm^{-1} that can be readily assigned to the carbonyl groups of the dithiolene ligand.[46] Owing to the presence of two Mo═O bonds in the syn conformation in compounds $(n\text{-}Bu_4N)_2[\mathbf{2}-\mathbf{6}]$, two bands are expected around 950 cm^{-1} as a result of the asymmetric and symmetric stretching modes. $\nu(M{=}O)_{asym}$ is typically strong in the infrared spectra[50] and appears in the 943−960 cm^{-1} range for complexes $(n\text{-}Bu_4N)_2[\mathbf{2}-\mathbf{6}]$. $\nu(M{=}O)_{sym}$ is identified as a medium peak in the Raman spectra of related compounds[50,58] and appears as a medium band in the Raman spectra of complexes $(n\text{-}Bu_4N)_2[\mathbf{2}-\mathbf{5}]$ between 932 and 957 cm^{-1}. In general, the C═C, C—S, and M═O vibration frequencies remain largely unchanged in the series $(n\text{-}Bu_4N)_2$-$[\mathbf{2}-\mathbf{6}]$. Minor differences are observed below 400 cm^{-1} that involve the metal−chalcogenide bonds.

ESI-MS and CID Spectra of $(n\text{-}Bu_4N)_2[M_2O_2(\mu\text{-}Q)_2$-$(dithiolene)_2]$ (M = Mo, W; Q = S, Se). Molecular analysis by MS has greatly benefited from development of ESI because it allows pre-existing molecules in solution to be gently transferred to the gas phase. ESI-MS and its tandem version ESI-MS/MS are rapidly becoming the techniques of choice for solution mechanistic studies in chemistry and biochemistry and for high-throughput screening of homogeneous catalysis reactions.[59−63] Applications to a number of inorganic and organometallic systems have demonstrated the versatility of the technique.[64−66]

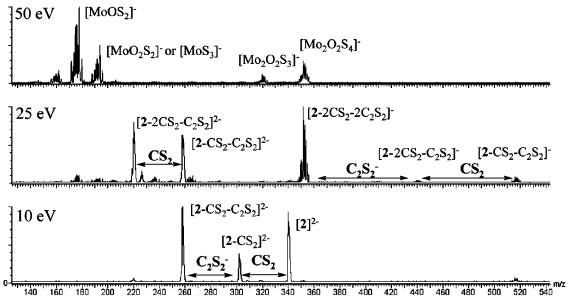

Figure 4. CID mass spectra at increasing CEs for the anion compound $[Mo_2O_2(\mu\text{-}S)_2(dmit)_2]^{2-}$ ($[\mathbf{2}]^{2-}$). The most intense fragmentation peak due to $C_2S_2^-$ (m/z = 88 amu) is not shown to bring the remaining species into a suitable scale.

In this work we have studied the CID mass spectra of the series of dinuclear cluster complexes $(n\text{-}Bu_4N)_2[\mathbf{2}-\mathbf{6}]$ in the 20−1020 m/z range using acetonitrile as the solvent. In the scan mode, the base peak of pure complexes corresponds to the molecular dianion $[M_2O_2(\mu\text{-}Q)_2(dithiolene)_2]^{2-}$ (dithiolene = dmit, dmid). All dmit derivatives show identical fragmentation pathways where the relative fragmentation peak intensities are independent of both the nature of the metal and the chalcogen incorporated. These experimental observations indicate similar $M-S_{dmit}$ binding energies for the $[\mathbf{2}-\mathbf{5}]^{2-}$ dianions and, in consequence, similar stabilities in the gas phase which in turn agree with the similar reactivities found in solution for compounds $(n\text{-}Bu_4N)_2[\mathbf{2}-\mathbf{5}]$. Figure 4 shows the CID spectra of compound $(n\text{-}Bu_4N)_2[\mathbf{2}]$ together with the peak assignment. An analogous behavior is observed for all complexes within the $[\mathbf{2}-\mathbf{5}]^{2-}$ dianion family.

At a low CE (10 eV) four major peaks emerge together with that of the parent dianion $[Mo_2O_2(\mu\text{-}S)_2(dmit)_2]^{2-}$ ($[\mathbf{2}]^{2-}$). A partial rupture of the dmit ligand with the evolution of neutral CS_2 produces the dianionic species $[\mathbf{2}-CS_2]^{2-}$ (m/z = 302). Further breaking of the ligand gives rise to $[\mathbf{2}-CS_2-C_2S_2]^{2-}$ (m/z = 258), the low abundant ion $[\mathbf{2}-CS_2-C_2S_2]^-$ (m/z = 516), and the nonmetallic fragment $[C_2S_2]^-$ (m/z =

(55) Rohmer, M.-M.; Bénard, M. *C. R. Chim.* **2005**, *8*, 1093.
(56) Fourmigué, M. *Acc. Chem. Res.* **2004**, *37*, 179.
(57) Liu, G.; Fang, Q.; Xu, W.; Chen, H.; Wang, C. *Spectrochim. Acta, Part A* **2004**, *60*, 541.
(58) Ueyama, N.; Nakata, M.; Araki, T.; Nakamura, A.; Yamashita, S.; Yamashita, T. *Inorg. Chem.* **1981**, *20*, 1934.
(59) Cooks, R. G.; Zhang, D. X.; Koch, K. J.; Gozzo, F. C.; Eberlin, M. N. *Anal. Chem.* **2001**, *73*, 3646.
(60) Takats, Z.; Nanita, S. C.; Cooks, R. G. *Angew. Chem., Int. Ed.* **2003**, *115*, 3645.
(61) Sabino, A. A.; Machado, A. H. L.; Correia, C. R. D.; Eberlin, M. N. *Angew. Chem., Int. Ed.* **2004**, *43*, 2514.
(62) Volland, M. A. O. V.; Adlhart, C.; Kiener, C. A.; Chen, P.; Hofmann, P. *Chem.—Eur. J.* **2001**, *7*, 4621.
(63) Chen, P. *Angew. Chem., Int. Ed.* **2003**, *42*, 2832.
(64) Henderson, W.; Nicholson, B. K.; McCaffrey, L. J. *Polyhedron* **1998**, *17*, 4291.
(65) Fong, S. W. A.; Yap, W. T.; Vittal, J. J.; Henderson, W.; Hor, T. S. A. *J. Chem. Soc., Dalton Trans.* **2002**, 1826.
(66) Toma, S. H.; Nikolau, S.; Tomazela, D. M.; Eberlin, M. N.; Toma, H. E. *Inorg. Chim. Acta* **2004**, *357*, 2253.

Scheme 2. Fragmentation Paths for the $[\mathbf{2}-\mathbf{5}]^{2-}$ Series at Different CEs[a]

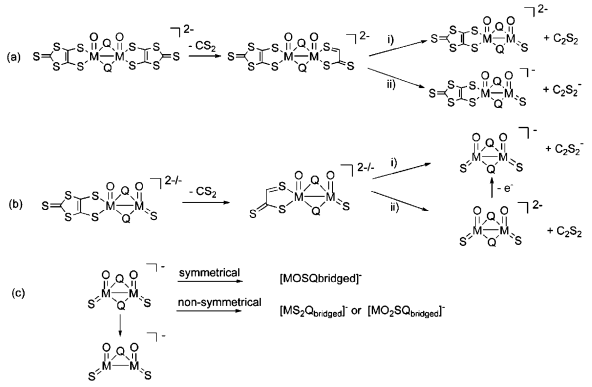

[a] (a) CE = 10 eV, (b) CE = 25 eV, (c) CE = 50 eV.

88). These observations imply the existence of two competitive fragmentation channels: (i) $[\mathbf{2}-CS_2]^{2-} \rightarrow [\mathbf{2}-CS_2-C_2S_2]^{2-} + C_2S_2$ and (ii) $[\mathbf{2}-CS_2]^{2-} \rightarrow [\mathbf{2}-CS_2-C_2S_2]^{-} + [C_2S_2]^{-}$ (see Scheme 2a). In this last pathway, charge splitting accompanies the ligand rupture. Increasing the CE to 25 eV results in the breaking of the other dmit ligand that again starts evolving CS_2 to give the corresponding $[\mathbf{2}-2CS_2-C_2S_2]^{2-}$ and $[\mathbf{2}-2CS_2-C_2S_2]^{-}$ anions (see Scheme 2b). The next fragmentation produces the single-charged $[\mathbf{2}-2CS_2-2C_2S_2]^{-}$ and $[C_2S_2]^{-}$ species. At this moment, tandem MS analyses of the doubly charged species $[\mathbf{2}-2CS_2-C_2S_2]^{2-}$ were carried out. This dianionic species was generated by "in-source" fragmentation at 35 V, and its fragmentation was induced in the hexapole. Only two fragments are seen in the CID spectra, namely, $[\mathbf{2}-2CS_2-2C_2S_2]^{-}$ and $C_2S_2^{-}$, and the fragmentation mechanism proposed is shown in Scheme 2b. Remarkably, in this case, only the monoanionic fragment $[\mathbf{2}-2CS_2-2C_2S_2]^{-}$ was observed as the metal-containing daughter peak. Again, two fragmentation channels are possible: (i) charge splitting accompanying the ligand rupture and (ii) the loss of neutral C_2S_2 and the formation of $[\mathbf{2}-2CS_2-2C_2S_2]^{2-}$ (see Scheme 2b). The higher Coulomb repulsion in this smaller doubly charged fragment $[\mathbf{2}-2CS_2-2C_2S_2]^{2-}$ explains its tendency to get oxidized and the fact that only the single-charged $[\mathbf{2}-2CS_2-2C_2S_2]^{-}$ ion could be detected. A similar mechanism has been proposed for the competitive symmetric fission and one-electron oxidation of several cuboidal Fe_4S_4 cluster dianions. In these complexes CID conditions are drastic enough to cause the oxidation that produces singly charged complexes at the same time as inducing symmetric fission to yield dinuclear Fe_2S_2 clusters.[26]

Fragmentation of the dimeric cluster $[M_2O_2(\mu\text{-}Q)_2]^{-}$ (M = Mo, W; Q = S, Se) core is only observed at CEs above 50 eV. Under these conditions, a minor fragmentation channel associated with the loss of one sulfur or selenium bridging atom is first observed, $[Mo_2O_2(\mu\text{-}S)S_2]^{-}$ (m/z = 320 amu) for $[\mathbf{2}]^{2-}$. The major process occurs in the symmetric degradation channel of the dinuclear unit to give a dominating peak attributed to the $[MoOSS_{bridged}]^{-}$ motif. This fragmentation is also observed in complexes $[\mathbf{3}-\mathbf{5}]^{2-}$ and gives the $[MoOSSe_{bridged}]^{-}$ and $[WOSSe_{bridged}]^{-}$ species as represented in Scheme 2c. In all cases, peaks appearing at $MOSQ_{bridged}$ + 16 amu are also observed, and these could be tentatively associated to the isobaric $[MS_2Q_{bridged}]^{-}$ or $[MO_2SQ_{bridged}]^{-}$ fragments that result from a nonsymmerical dissociation of the dinuclear unit followed by some kind of rearrangement of the terminal oxygen or sulfur atoms.

The CID spectra of the compound $(n\text{-}Bu_4)_2[\mathbf{6}]$ are similar to those of complexes $(n\text{-}Bu_4)_2[\mathbf{2}-\mathbf{5}]$ except that the observed CS_2 evolution at 10 eV is now replaced by a simultaneous loss of CO and COS, thus, affording the dianions $[\mathbf{6}-CO]^{2-}$ and $[\mathbf{6}-COS]^{2-}$ at m/z = 309 and 293 amu, respectively. Peaks due to the $[C_2S_2]^{-}$ (m/z = 88 amu) and $[C_2S_3]^{-}$ (m/z = 120 amu) anions are also observed. The fragmentation of the second dmid ligand at 25 eV takes place in a manner similar to that observed for the first dmid ligand to finally afford the monoanionic species $[Mo_2O_2S_4]^{-}$ that further degrades at higher CEs to give the $[MoOSS_{bridged}]^{-}$ mononuclear single-charged anion. In general, the characteristics of the dissociation pattern of the dithiolate dmit or dmid ligands in these complexes is a reflex of their molecular organization and can be used as a tool for structural elucidation in related systems.

To validate this idea, we extended our CID studies to the trinuclear $(n\text{-}Bu_4)_2[\mathbf{1}]$ as a way to confirm its chemical architecture. It showed three identical sequential two-step breaks of its three dmit ligands upon increasing the CE up to 70 eV to afford finally the $[Mo_3S_4S_3]^{-}$ cluster unit. The most significant difference between compound $(n\text{-}Bu_4)_2[\mathbf{1}]$ and dimers $(n\text{-}Bu_4)_2[\mathbf{2}-\mathbf{6}]$ has to do with the stability of the cluster core. The trinuclear Mo_3S_4 unit remains unaffected up to 70 eV, whereas dimers $(n\text{-}Bu_4)_2[\mathbf{2}-\mathbf{6}]$ undergo symmetrical dissociation under identical conditions. The robustness of the M_3Q_4 cluster unit has also been observed for the trinuclear phosphino derivatives of the general formula $[M_3Q_4(diphos)_3X_3]^{+}$ (M = Mo, W; Q = S, Se; diphos = dmpe, dppe; X = Cl, Br).[67,68]

Comparison between Gas- and Condensed-Phase Reactivity. The existence of electron-detachment processes in the collision cell makes unreliable any precise analysis regarding the net charge of these clusters in the gas phase. Despite this limitation, some qualitative information can be extracted from the nature of the fragmentation ions. At first glance, it is interesting to note the strong tendency of the dmit or dmid ligand to undergo degradation rather than the typically observed loss of the full ligand. Another interesting point is the presence of M═S bonds in the fragments obtained after the degradation of the first and second dithiolene ligand, which are $[M_2O_2(\mu\text{-}Q)_2(S)(dithiolate)]^{2-}$ and $[MoO_2(\mu\text{-}Q)_2(S)_2]^{-}$, respectively. These Mo═S units have been proposed to be the reactive sites in the precursors used for the preparation of dithiolene complexes via electrophilic addition of alkynes. Therefore, it is not surprising to see the presence of such Mo═S motifs in the degradation products of complexes $[\mathbf{2}-\mathbf{5}]^{2-}$, as they represent the precursor of the parent ions. In addition, the environment around each molybdenum atom in these degradation inter-

(67) Estevan, F.; Feliz, M.; Llusar, R.; Mata, J. A.; Uriel, S. *Polyhedron* **2001**, *20*, 527.
(68) Llusar, R.; Uriel, S.; Vicent, C. *J. Chem. Soc., Dalton Trans.* **2001**, 2813.

mediates, $[M_2O_2(\mu\text{-}Q)_2(S)(\text{dithiolate})]^{2-}$ and $[MoO_2(\mu\text{-}Q)_2(S)_2]^-$, contains terminal M(O)═S functional groups which are known to react in solution with dipolar molecules such as $(RO_2CC)_2$, CS_2, and SO_2 and have also been invoked as key intermediates in the mechanism of certain Mo oxotransferases.[69] Although, in our study, the existence of these species is limited to the gas phase, closely related compounds, namely, $[Mo_2O_2(\mu\text{-}S)_2(S)(S_4)]^{2-}$ or $[Mo_2O_2(\mu\text{-}S)_2(S)_2]^{2-}$, have been structurally characterized by Coucouvanis et al.[70,71] Because the species generated in the gas phase can find their homologues in the condensed phase, the possibility of generating them easily in the ESI conditions provides an attractive alternative to obtain direct information about their basic structural identity through fragmentation studies. On the other hand, tandem mass experiments offer the great advantage of on-line purification of complex mixtures by selecting the desired ion in the first quadrupole and inducing fragmentation in the collision cell. In this context, the introduction of reactive neutral molecules in the collision cell can provide a rapid screening of the species involved in certain reactions where the resulting products are analyzed in the second quadrupole. This has been exemplified in this work through the gas-phase reactivity studies of complex $(n\text{-}Bu_4N)_2$[**1**], using air as the collision gas.

Finally, the gas-phase dissociation path described above for the $[M_2O_2(\mu\text{-}Q)_2(S)_2]^-$ dimers that give the $[MOSQ_{bridged}]^-$ mononuclear fragments closely resembles the reverse of the solution synthetic route used for the preparation of complexes with dinuclear $Mo_2(\mu\text{-}S)_2$ units. In solution, internal molecular redox processes involving mononuclear complexes, such as $[MoS_4]^{2-}$ or $Mo(O)(S)(\eta^2\text{-}S_2)$, produce symmetric condensation products formulated as $[Mo_2S_2(\mu\text{-}S)_2(S_2)_2]^{2-}$ and $[Mo_2O_2(\mu\text{-}S)_2(S_2)_2]^{2-}$, respectively.[24,72]

Conclusions

The series of $(n\text{-}Bu_4N)_2[M_2O_2(\mu\text{-}Q)_2(\text{dmit})_2]$ (M = Mo, Q = S), $(n\text{-}Bu_4N)_2$[**2**]; M = Mo, Q = Se, $(n\text{-}Bu_4N)_2$[**3**]; M = W, Q = S, $(n\text{-}Bu_4N)_2$[**4**]; M = W, Q = Se, $(n\text{-}Bu_4N)_2$[**5**]; and $(n\text{-}Bu_4N)_2[Mo_2O_2(\mu\text{-}S)_2(\text{dmid})_2]$ {$(n\text{-}Bu_4N)_2$[**6**]} complexes is easily obtained by the cluster fragmentation in air of the trinuclear $[M_3Q_4(\text{dmit/dmid})_3]^{2-}$ species. These cluster trimers can be accessed through the reduction of the disulfide bridges in the corresponding $[M_3Q_7(\text{dmit})_3]^{2-}$ (M = Mo, W; Q = S, Se) clusters or by the substitution of the outer ligand in the already formed Mo_3S_4 complexes. In contrast with the octahedral metal-coordination environment usually found for these Mo_3S_4 compounds, the metal atoms in $[Mo_3S_4(\text{dmit})_3]^{2-}$ ([**1**]$^{2-}$) are five-coordinated, always without considering the metal−metal bond. The presence of a vacant coordination site in these dithiolates would explain their higher reactivity toward O_2. The dianionic compound $(n\text{-}Bu_4N)_2$[**2**] is also conveniently prepared by the replacement of DMF molecules by dmit in the pre-assembled dimer $[Mo_2O_2(\mu\text{-}S)_2(DMF)_6]^{2+}$.

The crystal structures of $(n\text{-}Bu_4N)_2$[**2**], $(n\text{-}Bu_4N)_2$[**4**], $(n\text{-}Bu_4N)_2$[**5**], and $(n\text{-}Bu_4N)_2$[**6**] show a syn distribution of the oxygen atoms within the cluster $M_2(\mu\text{-}S)_2$ core. ESI mass analysis was shown to be a versatile technique for the monitoring and characterization of the products formed upon degradation. CID channels of each dianion were analyzed by MS/MS experiments at different CEs. For the [**1**−**6**]$^{2-}$ dianions, a dominant CID fragmentation pathway has been found that consists of a two-step breaking of each dithiolene ligand followed by a symmetric degradation of the metal dimer in the case of complexes [**2**−**6**]$^{2-}$. No degradation of the trinuclear Mo_3S_4 unit is observed for [**1**]$^{2-}$ under similar conditions, indicating a more robust cluster unit in comparison with its dinuclear oxidation products. Some parallelism between gas-phase and solution reactivity has been envisioned.

Acknowledgment. Financial support from the Ministry of Science and Technology of Spain (Grant BQU2002-00313), Fundació Bancaixa-UJI (Grant P11B2004-19), and Generalitat Valenciana (IIARCO/2004/161) is acknowledged. We also thank the Servei Central D'Instrumentació Cientifica (SCIC) of the University. Financial support to B.D. from the Ministry of Education and Research (France) and the DGA (France) is also gratefully acknowledged.

Supporting Information Available: X-ray crystallographic files in CIF format for complexes $(n\text{-}Bu_4N)_2$[**1**], $(PPh_4)_2$[**2**], $(n\text{-}Bu_4N)_2$[**2**], $(n\text{-}Bu_4N)_2$[**4**], $(PPh_4)_2$[**5**], and $(n\text{-}Bu_4N)_2$[**6**]. This material is available free of charge via the Internet at http://pubs.acs.org.

IC0508728

(69) Holm, R. H. *Coord. Chem. Rev.* **1990**, *100*, 183.
(70) Coucouvanis, D.; Hadjikyriacou, A.; Toupadakis, A.; Koo, S. M.; Ileperuma, O.; Draganjac, M.; Saliflogou, A. *Inorg. Chem* **1991**, *30*, 754.
(71) Hadjikyriacou, A. I.; Coucouvanis, D. *Inorg. Chem.* **1987**, *26*, 2400.
(72) Pan, W. H.; Harmer, M. A.; Halbert, T. R.; Stiefel, E. I. *J. Am. Chem. Soc.* **1984**, *106*, 459.